

New approach to enhanced heat exchange efficiencies at ultralow temperatures

D. Burton, R. C. M. Dow, and C. J. Lambert

Department of Physics, University of Lancaster, Lancaster LA1 4YB, United Kingdom

(Received 13 December 1985)

We examine the heat transfer between a sintered metallic powder and liquid ^3He at ultralow temperatures. With the combination of a renormalization-group approach with the Lanczos method, a microscopic model is analyzed to yield the low-frequency density of states $\rho(\omega)$ of the sinter. In the weak-coupling limit $\rho(\omega)$ possesses a pronounced low-frequency peak leading to an enhanced heat transfer coefficient at low temperatures. This enhancement is shown to occur when the ratio of the long-wavelength velocity of sound C_s in the sinter to its velocity C_b in the bulk metal is small and can be optimized by minimizing this ratio.

The aim of this report is to suggest a new approach to enhanced heat exchange efficiencies at ultralow temperatures. It has long been suggested that finite-size effects in sintered metallic powder heat exchangers lead to thermal transport anomalies at ultralow temperatures.¹⁻⁴ An important example is provided by the heat transfer coefficient κ between phonons in the sinter and liquid ^3He quasiparticles. This is defined by $\kappa = \dot{Q}/\Delta T$, where ΔT is the temperature discontinuity generated by a heat flux \dot{Q} . As the temperature T decreases, the dominant bulk phonon wavelength in the metal eventually exceeds a typical grain size L and κ exhibits a crossover from $\kappa \sim T^3$ to $\kappa \sim T$. Despite its importance to the cooling of liquid ^3He to the lowest temperatures currently available, no systematic study of the effect on κ of varying the initial sintering conditions has been performed. In this report we argue that thermal transport at ultralow temperatures depends crucially on the sintering process and demonstrate that further enhancement of κ is possible. In addition, we suggest simple experimental criteria for estimating κ from measurements performed at room temperature.

To illustrate the role of granularity in determining the magnitude of the heat transfer coefficient, consider the following result for κ , valid in the limit $k_B T/\epsilon_F \ll 1$, where ϵ_F is the Fermi energy of the ^3He quasiparticles:^{5,6}

$$\kappa = \kappa_0 \int_0^\infty d\omega \rho(\omega) y I(y) / [\exp(y) - 1]. \quad (1)$$

In this equation, $y = \hbar\omega/k_B T$, $\rho(\omega)$ is the average phonon density of states per grain, per atomic degree of freedom, and

$$I(y) = \int_{-\infty}^\infty dx \{ [1 + \exp(x)][1 + \exp(-x - y)] \}^{-1}. \quad (2)$$

For ^3He quasiparticles of mass m_H , the constant is given by

$$\kappa_0 \approx (18m_H^2 \kappa_B \epsilon_F^2 / \pi \hbar^2 \sigma) V / L^4, \quad (3)$$

where σ is the mass density of the bulk metal and V the macroscopic volume of the sinter.

To understand the effect of granularity it is useful to introduce the dimensionless frequency $\Omega = \omega/\omega_b$ and temperature $\tau = k_B T/\hbar\omega_b$, where $\omega_b = \pi C_b/L$ is the frequency at which the wavelength of a bulk phonon of velocity

C_b approaches a typical grain size. For $\Omega \gg 1$, Debye theory yields $\rho(\omega) = \pi\Omega^2/2\omega_b$ and, as a consequence, for $\tau \gg 1$, Eq. (1) predicts $\kappa = B\tau^3$, where

$$B = \frac{\pi}{2} \int_0^\infty dy y^3 I(y) / [\exp(y) - 1].$$

Similarly, in the limit $\Omega \ll 1$, if the number of grains per unit volume is $(\alpha L)^{-3}$, Debye theory yields $\rho(\omega) = \pi\Omega^2/2\omega_b C^3$, where $C = C_s/\alpha C_b$ with C_s the ultralong-wavelength velocity of sound in the sinter. The dimensionless parameter $\alpha \gtrsim 1$ depends on the detailed shape of both grains and pores within the sinter. For $\tau \ll 1$ this yields $\kappa = B\tau^3/C^3$. Hence, since $C < 1$ for a sintered metallic powder, mean-field theory suggests that the introduction of granularity leads to a low-temperature enhancement in the heat transfer coefficient. To explain the crossover to $\kappa \sim \tau$ in the region $\tau \approx 1$, Rutherford *et al.*⁵ proposed, that by analogy with the low-frequency density of states (DOS) found in other disordered systems,⁷ $\rho(\omega)$ approaches a constant at intermediate frequencies. This behavior near $\Omega = 1$ is probably typical of sinters in current usage. However, by analyzing in detail a simple microscopic model of a granular structure, we now argue that a much more desirable $\rho(\omega)$ exists which can lead to further enhancement of the heat transfer coefficient.

The microscopic model has been described in detail elsewhere⁸ and is obtained by adding granularity to a symmetric Born model. The atoms within each grain are represented by single degrees of freedom of mass m coupled by harmonic springs of strength γ , while the atoms on adjacent surfaces of neighboring grains i and j are coupled by springs of strength Γ_{ij} . The volume of grain i is $L_i^3 = (N_i a)^3$, where a is the lattice constant. Given the probability densities $P(L_i)$ and $P(\Gamma_{ij})$ for the grain sizes and intergrain couplings, a dynamical matrix H can be constructed. Since each grain contains a large number (typically $\sim 10^9$) of high-frequency internal modes, the problem can be substantially reduced by performing a scale transformation.⁹ To this end one selects a cutoff Ω_{max} and eliminates all internal modes with frequency

$\Omega \geq \Omega_{\max}$. This yields a scaled dynamical matrix \tilde{H} describing the coupling between the remaining low-lying modes, which can be analyzed using standard numerical techniques. The results shown in Fig. 1 were obtained by employing an implementation of the Lanczos method¹⁰ due to Parlett and Reid¹¹ to yield the eigenfrequencies of \tilde{H} .

No detailed information is available for the probability densities of the grain sizes and couplings in a sintered metallic powder. However, in view of the size distribution found in other granular structures^{12,13} the following Γ distribution of the grain sizes was employed:

$$P(\xi_i) = [(g-1)!]^{-1/2} g^g \xi_i^{g-1} \exp(-g\xi_i),$$

where $\xi_i = (L_i/L)^3$. For such a distribution $L = \langle L_i^3 \rangle^{1/3}$ and $\sigma_L = \langle (\xi_i - 1)^2 \rangle^{1/2} = g^{-1/2}$. The intergrain couplings were chosen to have a simple rectangular distribution of the form

$$P(\Gamma'_{ij}) = \begin{cases} 1 & \text{for } 0.75\Gamma' \leq \Gamma'_{ij} \leq 1.25\Gamma', \\ 0 & \text{otherwise,} \end{cases}$$

where $\Gamma'_{ij} = L\Gamma_{ij}/\gamma a$ and $\Gamma' = \langle \Gamma'_{ij} \rangle$. In order to circumvent restrictions on computer time and storage, each plot of $\rho(\omega)$ shown in Fig. 1 was obtained in two stages. In the frequency range $0 \leq \Omega \leq 1.2$ the numerical analysis was performed on an array of 6^3 grains with periodic boundary conditions, with a cutoff of $\Omega_{\max} = 2$. For $\Omega > 1.2$, where the eigenstates do not deviate appreciably from the internal modes of the grains, the analysis was performed on an array of 2^3 grains with $\Omega_{\max} \approx 3.1$.

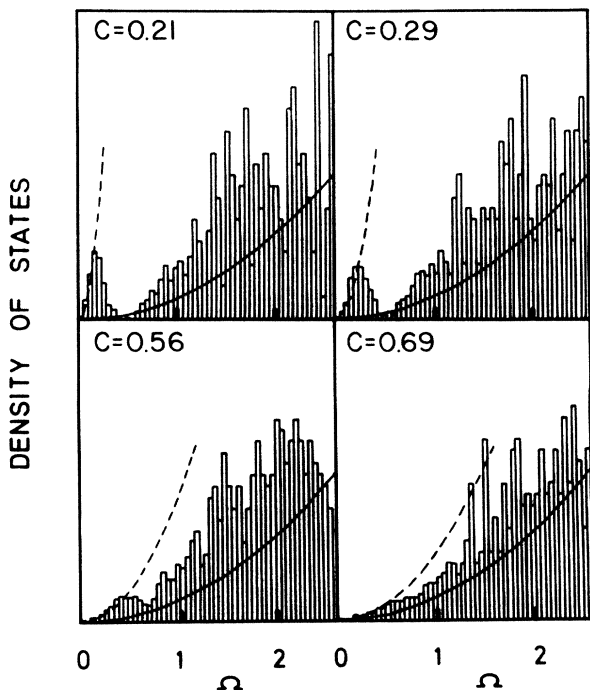


FIG. 1. Results for the density of phonon states $\rho(\omega)$ as a function of the dimensionless frequency $\Omega = \omega/\omega_b$. The solid line shows the high-frequency prediction $\rho(\omega) = \pi\Omega^2/2\omega_b$. The dashed line shows the ultralow-frequency prediction $\rho(\omega) = \pi\Omega^2/(2\omega_b C^3)$. Results are shown for a variety of velocity of sound ratios.

Figure 1 shows results for $\sigma_L = 1$ and a range of Γ' . Note that the average grain size L^3 does not appear explicitly in the results. L merely fixes the absolute frequency and hence the temperature scale. For each set of results we have quoted a value for the velocity of sound ratio C . This is obtained from the formula¹¹ $C^2 = \delta/(1+\delta)$, where $\delta = \langle (\Gamma'_{ij})^{-1} \rangle^{-1}$. For comparison the solid line shows the Debye-theory prediction for the density of states of the bulk material, while the dashed line shows the ultralong-wavelength prediction for the DOS of the granular structure. As the velocity of sound ratio increases towards unity, the computed DOS approaches this line. At weaker couplings, the results show that granularity leads to an enhanced DOS at low frequencies.

The DOS enhancement in the weak-coupling limit arises from two distinct mechanisms. At $\Omega \geq 1$, the calculated DOS is greater than the Debye prediction by a factor of roughly 2. This can be understood by considering a collection of *isolated cubic* grains with a distribution of sizes. The separation of the lowest-frequency modes of a cube of volume L^3 with free end boundary conditions is $\Delta\omega = \pi C_b a/L$. This is to be contrasted with a level separation of $2\Delta\omega$ which arises in the presence of periodic boundary conditions and is more appropriate to Debye theory. At nonzero but weak couplings this effect persists and leads to the higher-frequency enhancement of $\rho(\omega)$ at $\Omega \geq 1$. It is interesting to note that a similar DOS enhancement is observed in spin glasses.¹⁴

Of more importance is the appearance of a low-frequency peak in $\rho(\omega)$ at $\Omega \leq 1$, whose position is sensitive to the value of C and can therefore be tuned by varying the initial sintering conditions. To understand this behavior, consider first the zero-coupling, zero-disorder limit, where $\rho(\omega)$ consists of a sequence of δ functions. As the disorder is switched on, the $\omega \neq 0$ δ functions corresponding to the internal degrees of freedom of isolated grains spread to form a continuous DOS which cuts off below $\Omega \approx 1$. In the absence of coupling, the $\omega = 0$ δ func-

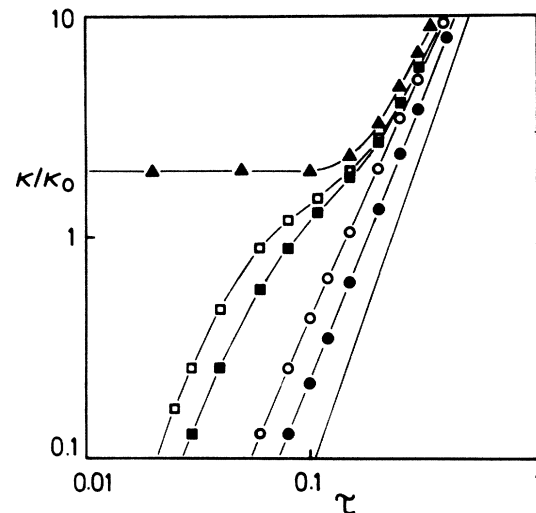


FIG. 2. Heat transfer coefficient κ versus dimensionless temperature $\tau = k_B T / \hbar\omega_b$. The solid line is for a velocity of sound ratio $C = 1$, the remaining curves are for the ratios $C = 0.69$ (●), $C = 0.56$ (○), $C = 0.29$ (■), $C = 0.21$ (□), and $C = 0$ (▲).

tion is unaffected, however. In the presence of very weak coupling this δ function spreads to form a band of states which is separated from the higher-frequency internal modes. The upper edge of this band is at $\Omega \approx C$.

To demonstrate the desirability of such a low-frequency peak, we have evaluated the heat transfer coefficient κ , by combining Eq. (1) with the results of Fig. 1. This yields the κ versus τ curves shown in Fig. 2. For $C \approx 1$, κ exhibits a simple T^3 dependence and for $C \approx 0.1$, κ is approximately linear in the range $0.07 < \tau < 0.15$. However, for smaller C , κ possesses a shoulder of magnitude $\lesssim \kappa_0 I(0)$ over a limited temperature range.

These results clearly demonstrate that at small τ the magnitude of κ is extremely sensitive to the value of C and hence to the initial sintering conditions. There are

two parameters of interest, both of which can be obtained experimentally from measurements performed at room temperatures. The first is the velocity of sound ratio C . If C is less than roughly 0.5 then the magnitude of κ is significantly enhanced. The second parameter is the average grain size L , which for a given value of τ fixes the absolute temperature. It is important to note that L is not necessarily the grain size of the unsintered powder. Electron micrographs reveal that a typical sinter consists of tightly bound clusters of powder particles which are loosely coupled together to form the sinter. It is the size of these clusters to which L refers.

The authors wish to thank the Science and Engineering Research Council for financial aid.

¹J. P. Harrison and D. B. McColl, *J. Phys. C* **10**, L297 (1977).

²N. Nishiguchi and N. Nakayama, *Phys. Rev. B* **25**, 5720 (1982).

³N. Nishiguchi and N. Nakayama, *Solid State Commun.* **45**, 877 (1983).

⁴J. P. Harrison, *J. Low Temp. Phys.* **37**, 467 (1979).

⁵A. R. Rutherford, J. P. Harrison, and M. J. Scott, *J. Low Temp. Phys.* **55**, 157 (1984).

⁶G. A. Toombs, F. W. Sheard, and M. J. Rice, *J. Low Temp. Phys.* **39**, 273 (1980).

⁷R. C. Zeller and R. O. Pohl, *Phys. Rev. B* **4**, 2029 (1971).

⁸C. J. Lambert, *J. Low Temp. Phys.* **59**, 123 (1985).

⁹D. Burton, R. C. M. Dow, and C. J. Lambert, *J. Phys. C* (to be published).

¹⁰R. Haydock, *Solid State Phys.* **35**, 215 (1980).

¹¹B. N. Parlett and J. K. Reid (unpublished).

¹²D. Weaire and N. Rivier, *Contemp. Phys.* **25**, 59 (1984).

¹³T. Kiang, *Z. Astrophys.* **64**, 433 (1966).

¹⁴R. B. Grzonka and M. A. Moore, *J. Phys. C* **16**, 1109 (1983).

¹⁵D. Deptuck, J. P. Harrison, and P. Zawadzki (unpublished).